



Tehran University of Medical
Sciences Publication
<http://tums.ac.ir>

Iran J Parasitol

Open access Journal at
<http://ijpa.tums.ac.ir>



Iranian Society of Parasitology
<http://isp.tums.ac.ir>

Original Article

Nanoincorporation of Plumbagin in Micelles Increase Its in Vivo Anti-Plasmodial Properties

Hamid Rashidzadeh^{1,2}, Payam Zamani², Mahdi Amiri³, Seyed Mehdi Hassanzadeh⁴, *Ali Ramazani^{2,5}

1. Student Research Committee, Zanzan University of Medical Sciences, Zanzan, Iran
2. Department of Pharmaceutical Biomaterials, School of Pharmacy, Zanzan University of Medical Sciences, Zanzan, Iran
3. Departments of Medical Parasitology and Mycology, Zanzan University of Medical Sciences, Zanzan, Iran
4. Researches & Production Complex, Pasteur Institute of Iran, Tebran, Iran
5. Cancer Gene Therapy Research Center, Zanzan University of Medical Sciences, Zanzan, Iran

Received 20 Nov 2021

Accepted 19 Jan 2022

Keywords:

Plasmodium berghei;
Copolymers;
Micelles;
Plumbagin;
Sustained release

*Correspondence

Email:

ramazania@zums.ac.ir

Abstract

Background: The application of plumbagin (PLN), with a wide use in pharmaceutical science, is limited due to its low water solubility and poor bioavailability. Micelles can encapsulate hydrophobic drugs due to their hydrophobic core. The aim of this study was to develop and characterize a polymeric micelle formulation of PLN and evaluate its in vivo anti-plasmodial property.

Methods: The study was conducted at Zanzan University of Medical Sciences, Zanzan, Iran in 2018. The triblock copolymeric micelles of PLN was prepared by ϵ -caprolactone ring-opening polymerization, by PEG as the macroinitiator and using Sn(Oct)₂ for its catalytic properties. The synthesized nanoparticles were characterized by ¹H NMR, FTIR, GPC, AFM, and DLS. The encapsulation efficiency, drug loading capacity, and drug release were measured by UV-Vis at 520 nm. Also in vivo anti-plasmodial potential of fabricated drug loaded micelle was investigated using the 4-day suppressive test against *Plasmodium berghei* infection in mice.

Results: The nanoparticles average diameter was obtained less than 80 nm. The loading capacity and encapsulation efficiencies were 18.9±1.3% and 81±0.78%, respectively. In vitro, PLN release studies showed a sustained-release pattern until 7 days in PLN-loaded micelles (M-PLN) and drug release rate in acidic condition was higher than neutral condition. In vivo, anti-plasmodial results against *P. berghei* displayed an 8-fold increase in anti-plasmodial activity of M-PLN when compared to free PLN at the tested dosage level on the 7th day.

Conclusion: Based on these results, PCL-PEG-PCL micelles have a great potential to be the carrier for PLN for the malaria targeting.



Copyright © 2022 Rashidzadeh et al. Published by Tehran University of Medical Sciences.

This work is licensed under a Creative Commons Attribution-NonCommercial 4.0 International license.

(<https://creativecommons.org/licenses/by-nc/4.0/>). Non-commercial uses of the work are permitted, provided the original work is properly cited

Introduction

Malaria is one of the life-threatening infectious diseases which still acts as the main cause of mortality and morbidity in tropical and subtropical regions of the world and the malaria-related death has increased from 18% in 2017 to 28% in 2018 which resulted in 0.435 million death (1). The malaria re-emerging is more vulnerable in the poorest countries that is due to increase resistance to the majority of current antimalarial drugs and vectors to insecticides (2-5).

Natural products play vital roles as important therapeutic substances for the prevention and therapies of chronic and infectious human diseases including cardiovascular disease, leishmaniasis, inflammation, diabetes, cancer, malaria (6) and toxoplasmosis (7). Plumbagin (5-hydroxy-2-methyl-1,4-naphthoquinone) (PLN), a plant-derived medicine, extracted from the roots of *Plumbago* plants, exhibit both anticancer and anti-plasmodial effects and its activity has been shown by using in vitro and in vivo studies. Furthermore, herbal products may offer relatively cheap and alternative therapy opportunities for malarial human diseases (8, 9).

Simonsen et al. reported the in vitro antimalarial activity against a chloroquine-sensitive clone of *P. falciparum* (3D7) by alcoholic extract of *Plumbago zeylanica*. The IC₅₀ (concentration that inhibits parasite growth by 50%) of this extract was 17 µg/ml (10). The malaria enzyme activity has inhibition to 50% via PLN at inhibitory concentrations of 5 µM (11). Recently, ethanolic extract of *P. indica* Linn have promising antimalarial activity (12).

Pharmacokinetics studies revealed restricted biopharmaceutical criteria such as water insolubility and high lipophilicity (log P 3.04), the oral bioavailability of PLN is only 39% (13). Drug solubility initially affect pharmacokinetics results such as, absorption data like its rate

and extent, therapeutic efficacy, and oral bioavailability (14). As the drug introduced into the clinical setting, it becomes essential to develop a formulation that significantly increases the solubility while potentially reducing systemic toxicity. Indeed, a proper formulation could advocate on patient compliance and achieve optimal therapeutic potential (15-18).

The possibility of hydrophobic drugs encapsulation is assured progress to develop the intravenous drug formulation (19). For loading the hydrophobic drugs, the amphiphilic nanoparticles use a hydrophilic shell with hydrophobic core are of tremendous applicants (20). Poly (ε-caprolactone)-poly (ethylene glycol)-poly (ε-caprolactone), tri-block copolymer, are self-assembled nanoparticles: a PEG as a hydrophilic shell with PCL for hydrophobic core (21).

The aim of this study was to determine the preparation of PLN encapsulated PCL-PEG-PCL micelles and investigation of its in vivo anti-plasmodial activity.

Materials and Methods

The study was conducted in Zanzan University of Medical Sciences, Zanzan, Iran in 2018. Chloroquine (CQ) were purchased from Sigma Co. (Germany), PEG (Mn=6000Da) (Aldrich, St. Louis, USA, CAS.9004744), stannous 2-ethyl-hexanoate (Sn(Oct)₂) (Aldrich, St. Louis, USA, CAS. 301100), ε-caprolactone (97% purity) (Aldrich, USA, CAS. No 502443), PLN (Sigma-Aldrich, USA), ethanol, acetone, and all reagents and chemicals used in this work were analytical grade.

Synthesis of PCL-PEG-PCL triblock copolymers

The PCL-PEG-PCL triblock copolymers were prepared according to our previous study (22).

PCL-PEG-PCL copolymers Characterization

The triblock copolymer's chemical structure and composition were evaluated by Fourier transform infrared spectroscopy (FTIR) (Bruker, Tensor 27, USA) and proton nuclear magnetic resonance spectroscopy (¹HNMR) in CDCl₃ at 400 MHz (Bruker, Avance 400, USA). The differential scanning calorimetry (DSC) (Mettler Toledo, model Star SW 9.30, Selangor, Switzerland) was used for thermal analysis. Gel permeation chromatography (GPC) (Knauer, Berlin, Germany) set with a differential refractometric detector and an ultrastyrigel column (4.6 × 30 mm) (Waters, Milford, USA, model HR 4E, USA) was used to average molar mass determination and distribution of the copolymers. Tetrahydrofuran (THF), mobile phase, with a flow-rate of 1 mL/min and the injection volume of 50 μL of stock solutions (0.1-0.5 w/v%) were used. In addition, the copolymer was further characterized by relative elution time to polystyrene monodisperse standards in the range of 1.500-35.500 kDa (Varian Palo Alto, CA, USA).

PLN-loaded micelles Preparation

For synthesizing the desired micelles, nano-precipitation method was applied. Briefly, 20 mg PCL-PEG-PCL copolymer and 6 mg PLN were dissolved in 2 mL acetone. The solution containing copolymer, drug, and organic solvent were injected drop-wise through a syringe (G=22) into 25 mL distilled water under stirring at 25°C. The micelles formation will be completed by the disappearance of the organic solvent. The unloaded PLN will be removed by acetone eliminating with rotary vacuum evaporation at 35°C and the filtration of resultant aqueous solution throughout a 0.45 μm filter membrane. Micelles were centrifuged (20000 g) for 20 min and final powder form produced by freeze-dried at 14 Pa and -78 °C (EYELA, 2100, Tokyo, Japan) for residual solvent elimination.

Micelles Characterization

Particle morphology

Morphology of developed micelles were assessed by Atomic force microscopy (AFM) (JPK, Berlin, Germany, model Nano Wizard).

Measuring Particle size

Dynamic light scattering (DLS) with nano/zetasizer was used for micelle mean particle size and particle size distribution study (Malvern Instruments, Worcestershire, UK, model Nano ZS).

Micelles Stability

Physical stability studies of the micelles, the size distribution of the nano-dispersion was monitored in PBS (pH 7) solution at time periods of 0, 7, 28, 56, 140, 112 and 168 days after preparation, while the samples were kept at 37 °C.

Loading efficiency Determination

Micelles drug entrapped evaluation were carried out by determining the drug loading capacity (LC) and drug encapsulation efficiency. Loading capacity (LC) was calculated as:

$$\%LC = \frac{W_{drug}}{W_{micelles}} \times 100$$

[1]

%LC, indicative of the loading capacity, $W_{micelles}$ and W_{drug} represent the amount of micelle weight and drug entrapped into the micelle, respectively. The concentration of entrapped the measurement of PLN into the micelles was carried out by UV-Vis Spectrometer at 420 nm (Thermo Fisher Scientific, USA, Madison, model GENESYS™ 10S).

Micelle Encapsulation efficiency (EE) was determined as:

$$EE\% = \frac{(\text{weight drug in micelles})}{\text{weight of initial drug}} \times 100$$

[2]

FTIR analysis

Any possible drug-copolymer interactions were studied by the FTIR analysis, the mi-

celles spectrum were compared with pure drug and polymers.

Thermal analysis

DSC analysis applied to understand the relationship of drug and copolymer and any interactions between drug and copolymer. The analysis performed on free PLN, triblock copolymer and M-PLN. The heating rate was $10\text{ }^{\circ}\text{C min}^{-1}$ and data were recorded from 0 to $200\text{ }^{\circ}\text{C}$.

In vitro drug release study

Dialysis bag method was applied in order to study the PLN release from the micelles. Briefly, 5 mg freeze-dried M-PLN were dispersed in phosphate-buffered saline (PBS) (2 mL) containing 5% (v/v) tween 80 as a donor medium and micelles were suspended in dialysis bag (Mw 12 kDa) and incubated at $37\text{ }^{\circ}\text{C}$ with a gentle shaking of 200 rpm and immersed in 15 mL PBS as a receptor medium. At a specified time intervals, 1 mL sampling is carried out in the receptor medium and simultaneously replaced by 1 mL fresh PBS to maintain the sink condition. The concentration of released PLN in the receptor medium was evaluated with UV-Vis at 520 nm. Release studies were performed in triplicate. Averaged obtained data were used to calculate the amount of free PLN. The cumulative amount of PLN released was plotted versus time (during 168 hours).

In vivo anti-plasmodial assay

In vivo anti-plasmodial activity of M-PLN was evaluated using the 4-day suppressive test against *P. berghei* infection in mice (2, 21). The *P. berghei* ANKA strain was kindly provided by Pasteur Institute of Iran. In the current study 25 female Swiss albino mice, weighing 20–25 g, were categorized into five groups (untreated or control, M-PLN, bared micelles, CQ and PLN). The dosage used for CQ, PLN, M-PLN and free micelles was 5, 20, 105.82 (containing 20 mg PLN) and 86.92 mg/kg, respectively.

On the first day of the experiment, each mice in every group received 1×10^6 *P. berghei* (ANKA) infected red blood cells (RBCs) by intraperitoneal injection. Groups of five mice were dosed daily by intraperitoneal injection for 4 successive days and a blood smear was taken on day fifth and seventh of the test. Following staining of smears with Giemsa stain, the suppression of parasitemia and percent of growth were determined for each treatment group by comparison the parasitemia (by enumeration of 3000 RBCs) present in infected controls with those in test animals. Chloroquine (CQ) as a positive control and carrier solvent as the negative control were used.

This project was conducted in accordance with the approval of the Institutional Animal Ethical Committee of Zanjan University of Medical Sciences (Ethical code: ZUMS.REC.1394.3271).

Results

PCL-PEG-PCL copolymer Synthesis and characterization

The composition and structure of the synthesized polymeric carrier was assigned by ^1H NMR spectroscopy in CDCl_3 as solvent. In HNMR spectrum of copolymers, the observation of chemical shifts at 1.61 ppm, 1.72 ppm, 2.43 ppm, and 4.11 ppm were allocated to the methylene's (CH_2) of PCL. As well as, the chemical shift of methylene protons which present in methylene (CH_2) groups of PEG was also observed at 3.84 ppm. The Characteristics of the synthesized triblock copolymers are reported in Table 1. In the FTIR spectrum of synthesized copolymers, the observation of sharp and intense bands at 1111.81 cm^{-1} and 1725.26 cm^{-1} can be assigned to the presence of ether (C–O) and carboxylic ester (C=O) groups, respectively; thereby indicating that PCL-PEG-PCL is synthesized. Moreover, GPC results revealed that the weight-based average molar mass of PCL-PEG-PCL triblock copolymer was 16432 Da

which is shown in Table 1. The presence of the endothermic peak at 51.32 °C in the DSC thermogram of PCL-PEG-PCL indicates that

the peaks of PEG and PCL are merged together.

Table 1: Molecular characteristics of the synthesized copolymers

Copolymer	PEG M_w (g/mol)	CL/ EG feed	M_n (Da) ^a	M_w (Da) ^a	PdI ^b	T_m (°C) ^c	DP_{PEG}	DP_{PCL}^d
PCL-PEG-PCL	6000	2	14927	16432	1.10	51.32	136.36	91.39

a: Determined by GPC analysis using narrow molecular weight polystyrene standards.

b: M_w/M_n = Dispersity index of the polymers (PdI) determined by GPC analysis

c: Calculated from the first run of DSC as half of the extrapolated tangents

d: DP: degree of polymerization

Copolymeric micelles: Preparation and characterization

The confirmation for micelles formation was carried out by AFM. The prepared micelles exhibited a spherical morphology with a homogeneous dispersion and their size were approximately 63 nm (Fig. 1). Also, the particle size and particle size distribution of mi-

celles were determined by dynamic light scattering technique (DLS), with values of 78 and 0.23 respectively (Fig. 2). Moreover, the zeta potential of the prepared micelle was -5.37 mV which is shown in Fig. 2. The drug loading and entrapment efficiencies of prepared micelle were determined, with values of $18.9 \pm 1.3\%$ and $81 \pm 0.78\%$, respectively.

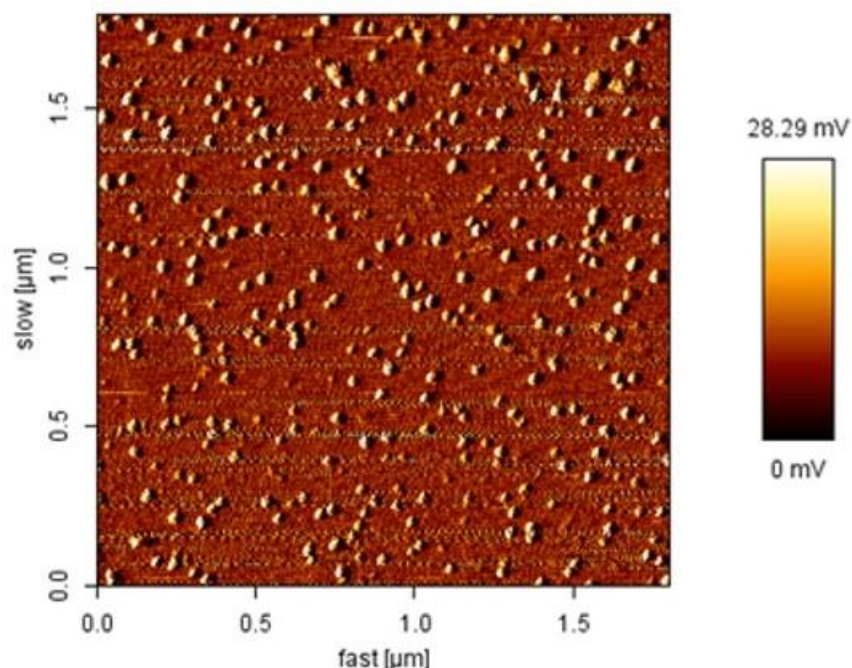


Fig. 1: AFM image of PLN loaded spherical core shell PCL-PEG-PCL micelles

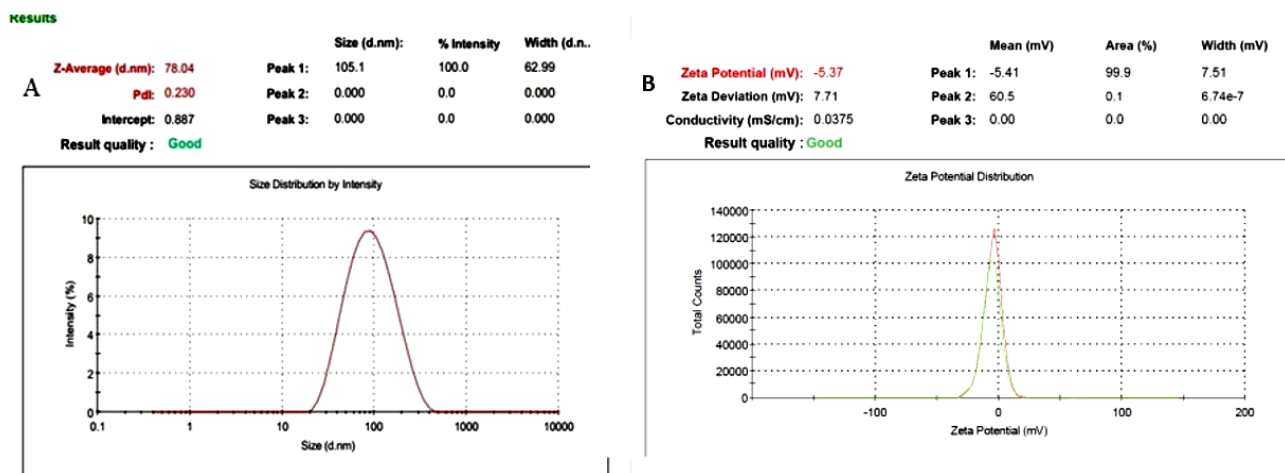


Fig. 2: Particle size distribution and ζ -potential of PLN loaded PCL-PEG-PCL micelles: (A) particle size distribution of PLN loaded PCL-PEG-PCL micelles, (B) ζ -potential

Physical stability of micelles

The stability of M-PLN has been tested during the study period of 168 days. The change in particle size of M-PLN in relation to incubation time is illustrated in Fig. 3. The average

size of M-PLNs was increased slightly. However, this observation could not be considered as an aggregation since the aggregation usually leads to increases to several folds.

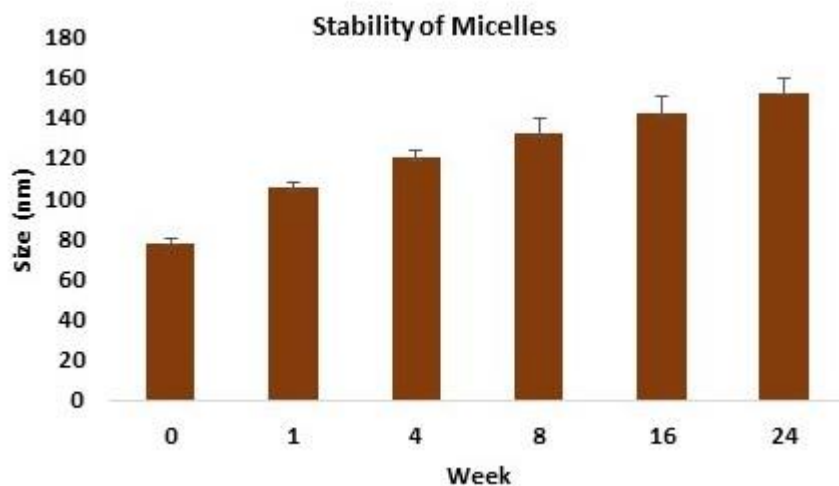


Fig. 3: Physical stability of PLN loaded PCL-PEG-PCL micelles by monitoring the size distribution in 168 days

FTIR analysis

The possibility of drug-copolymer interaction as well as, confirmation on micelles drug loading, was evaluated by comparison of the FTIR spectra (Fig. 4). The intense bands at 3459 cm^{-1} are related to the O-H stretching,

also peaks observed at 1652 cm^{-1} is assigned to the C=C stretching and the peaks observed in the area of 853.33 cm^{-1} related to the C-H stretching aromatic ring of PLN. The FTIR spectra of the synthesized PCL-PEG-PCL was shown in Fig.4.

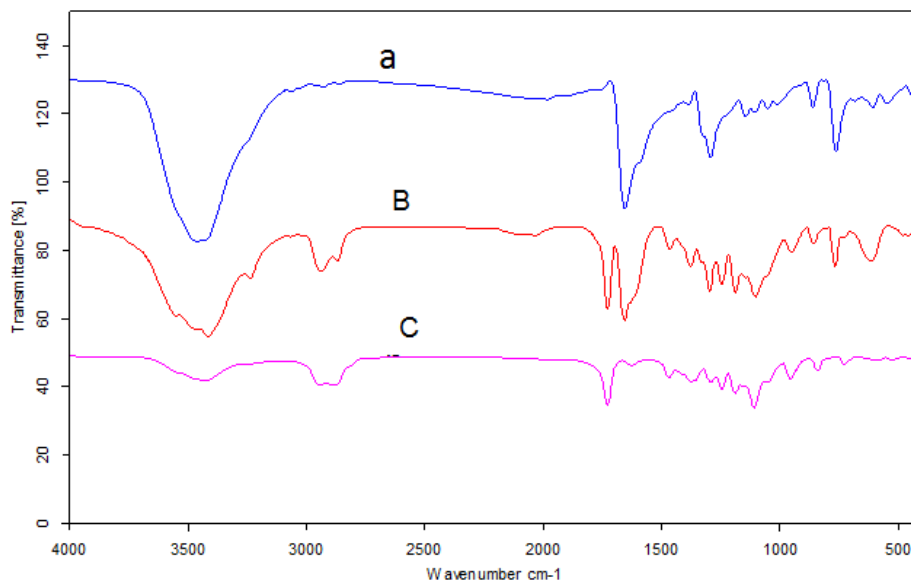


Fig. 4: FT-IR spectra of (a) PLN and, (b), PCL-PEG-PCL, (c) PLN loaded PCL-PEG-PCL micelles

DSC analysis

DSC thermograms as one of the thermoanalytical techniques, corresponding to triblock copolymer (PCL-PEG-PCL) is shown in Fig. 5. The triblock copolymer thermogram exhibited an endothermic peak at 51.32 °C which indicates the melting of the crystalline portion

of the triblock copolymer (PCL). The DSC thermogram of PLN showed an endothermic peak at 147.70 °C whereas M-PLN displayed endothermic peaks at 49.83 °C which is an indication of the melting process of PCL-PEG-PCL and PLN in these micelles.

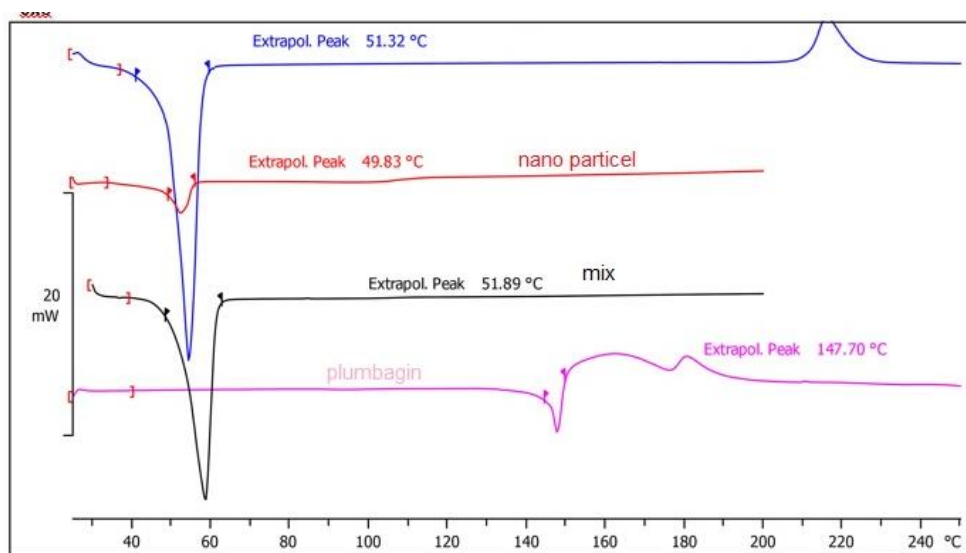


Fig. 5: DSC thermograms of (a) PCL-PEG-PCL copolymer, (b) physical mixture of PCL-PEG-PCL copolymer and PLN, (c) PLN loaded PCL-PEG-PCL micelles, and (d) PLN

In vitro release of PLN

The drug release profile of free PLN was investigated to confirm the drug molecules diffusion through the dialysis layer. Free PLN was showed rapid release profile and reached its peak at 84.00% and 82.30% in the first 10 hours at pH 5.5 and 7.4, respectively. This clearly indicated that there is no barrier to the diffusion of PLN molecules across the dialysis layer. Fig. 6 depicted the release profiles of PLN from the drug-loaded micelles at pH 5.5 and 7.4. As expected, any significant initial burst release profile of PLN could not be reported. The PLN release percentage from the micelles could be determined in Fig. 6. After incubation of M-PLN under the sink condition at 37°C for 72 h, the amounts of PLN released in the media with pH 7.4 and 5.5

were approximately 48.00, and 54.70%, respectively. The common reason for this experience is attributed to the sensitivity of the release profile to pH of PLN from the micelles since the copolymer is degraded in acidic pH condition by hydrolysis of the polymer backbone. Also, the release curve of PLN is faster in acidic condition than in neutral, as in acidic environment, the polymer is protonated and causes polymer matrix to swell. In fact, this phenomenon is really desirable in fields of drug delivery where they can potentially facilitate the release of drug from obtained micelles. The results indicated that the maximum PLN releases after a period of 120 h were 63.00, and 70.26 % respectively for PBS in pH 7.4 (neutral) and pH 5.5 (acidic condition).

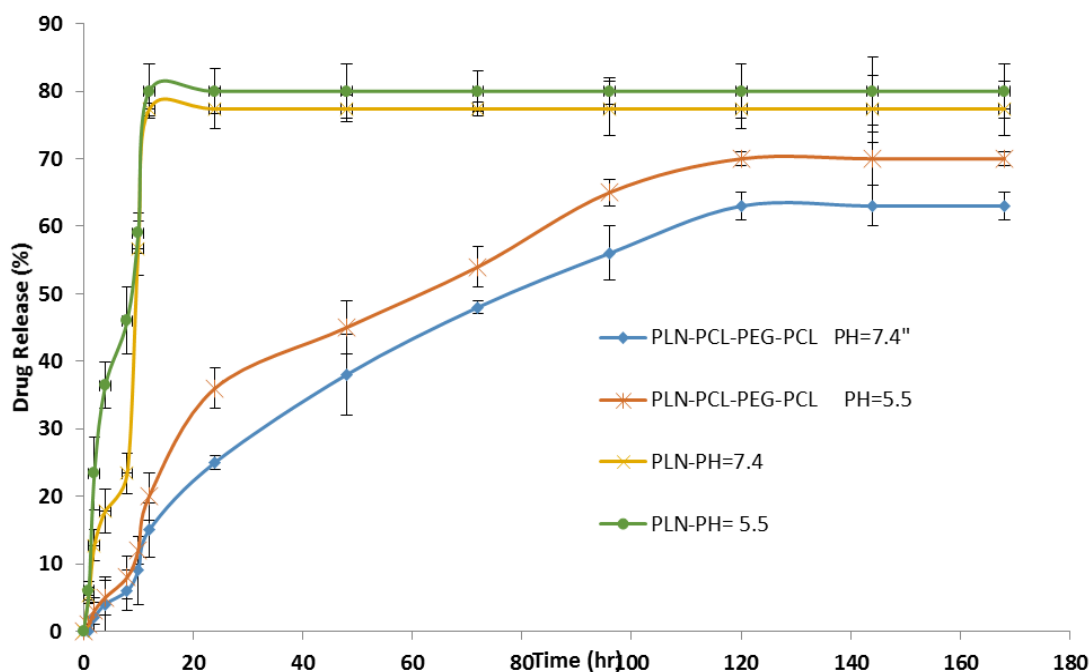


Fig. 6: The release profiles of PLN from PLN loaded micelles in different release media Data shows mean \pm SD (n = 3)

In vivo anti-plasmodial activity

Results of the 4-day suppressive in vivo anti-plasmodial property of M-PLN, PLN and bare micelle in comparison with standard drug CQ presented in Fig. 7. As indicated in Fig. 7, M-

PLN effectively causes inhibition of the parasite growth compare to free PLN and bare micelle (1.58% parasitemia versus 2.14 and 2.25%) at the same dose. Besides, the M-PLN have sustained drug release behavior and im-

proved the blood circulation time compared to free drug, hence the M-PLN more suppressed the parasite growth. The therapeutic application of PLN is limited due to its low aqueous solubility, hence it is necessary to develop drug carrier systems to improve its poor water solubility, bioavailability and overcome its limitations. Therefore by encapsulating the PLN in copolymeric micelles, the above-mentioned restrictions can be overcome. Similar to other nanocarriers, PCL-PEG-PCL could greatly enhance the water solubility and bioavailability of PLN. Therefore, the difference in antimalarial activity between M-PLN and PLN could be attributed to the difference

in their water solubility and blood circulation time. The percentage of suppression on the 7th day in the NC, M, and PLN treated groups is less than the 5th day, while for CQ and M-PLN, the percentage of suppression on the 7th day is more than the 5th day. With respect to decreasing the activity of parasitemia, the most potent antimalarial activity of CQ reported on 5th and 7th day. In addition, parasite depletion (%) of mice while treating with CQ (100%) and M-PLN (92.3%) was remarkably higher than the negative control group (0%) and the groups treating by M (9.2%), PLN (30.7%) ($P < 0.01$) on 7th day.

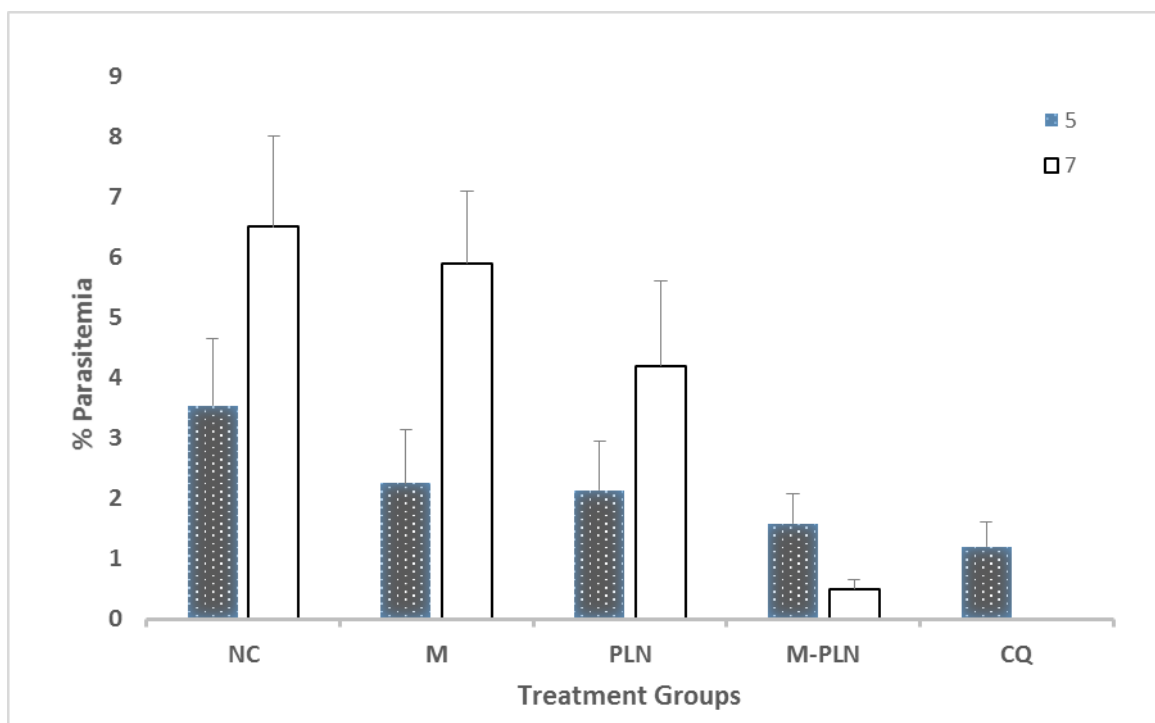


Fig. 7: In vivo anti-plasmodial property of M-PLN, PLN, CQ and bare micelles

Discussion

Malaria is still one of the life-threatening infectious diseases which its treatment and eradication are confronted with some challenges. Most of the chemotherapeutics that used as antimalarial agents are hydrophobic in nature like PLN (23). PLN has shown multi biological

characteristics as well as great anti-plasmodial properties but its application is extremely limited due to poor water solubility (24, 25).

In order to increase the solubility of poorly water soluble therapeutic agents nanotechnology based on polymeric micelles can be applied as a promising approach (26, 27). In this

regard, in the current study PLN was incorporated into PCL-PEG-PCL micelles to improve its water solubility. It is believed that pegylation could enhance the blood circulation time and alter the pharmacokinetics parameters and hence we applied PEG-PCL-PEG to encapsulate the PLN (22, 24, 28). After M-PLN was fabricated several techniques were employed to confirm the PLN was encapsulated successfully into PCL-PEG-PCL micelle. By comparing the resulting FTIR data of PLN with the drug-loaded micelles spectra, the presence of PLN characteristic peaks ($1200\text{--}1700\text{ cm}^{-1}$) can be deduced that the PLN is successfully loaded into the micelles (29). The shift in the micelles spectrum could be due to the possible interaction between PLN and C=O group of PCL-PEG-PCL (29). Moreover, in DSC thermogram the peak of M-PLN ($49.83\text{ }^{\circ}\text{C}$) probably supports a physical association between PCL-PEG-PCL and PLN after drug loading in micelles, due to this fact that the PCL melting point of micelles was lower than the melting point of desired PCL copolymer ($51.32\text{ }^{\circ}\text{C}$) and free PLN ($147.70\text{ }^{\circ}\text{C}$) (30). Physical stability (particle with no aggregation) is a critical factor which can alter the therapeutic efficacy of drugs.

In our study particle size was obtained with DLS during 24 weeks and the particle size was slightly increased. These changes in particle size can be attributed to the hydration or swelling of some portions of the copolymer as the hydrophilic PEG portions present in the backbone of M-PLN and aggregation was not take place (31). In vitro sustained release profile of PLN from the micelle can be attributed to the fact that PLN is trapped in the core of the micelles (32). Hence, these micelles can be considered as an attractive nano drug delivery carrier for controlled drug delivery for not only PLN but also for any hydrophobic drugs to aim a diverse therapeutic application. Due to the poor water solubility of PLN, it showed poor absorption and low bioavailability. In one study, PLN was encapsulated into a pegylated liposome and introduced to the

mice, the result indicated that the fabricated formulation could serve as a promising parenteral platform for PLN with enhanced plasma half-life and therapeutic efficacy in comparison with free PLN (33).

In our study, the order of suppression is as follows: CQ > M-PLN > PLN > M > NC this may attributed the sustained release of PLN from micelle which could provide better absorption condition and prolonged blood circulation time. These results proposed that the micelles could efficiently increase the solubility and bioavailability of free PLN.

Conclusion

M-PLN were successfully synthesized by ring opening polymerization (ROP). Micelles were specified and compared in relation to, particle morphology, particle size, zeta potential, polydispersity index, drug-loading capacity, and drug entrapment efficiency. The results clearly indicate that the stable nanoparticles with the nanoscale size and narrow polydispersity index as well as negative zeta potential were obtained. The drug-loading capacity and drug entrapment efficiency were high enough and satisfactory for drug delivery. The particles showed spherical shape morphology and the profile of drug release showed a sustained-release with a pH-dependent pattern. M-PLNs provided an appropriate and acceptable method for in vivo delivery of PLN to *P. berghei* infected erythrocytes. This developed nano-drug delivery system could be applied as a promising candidate drug for introducing in clinical settings after clinical trials.

Acknowledgements

This study was financially supported by Zanjan University of Medical Sciences.

Conflict of interest

The authors declare no conflicts of interest associated with current study.

References

1. Organization WH. World malaria report 2018 (world health organization, geneva, switzerland, 2018). 2018. <https://www.who.int/publications-detail-redirect/9789241565653>
2. Ramazani A, Hamidnezhad R, Foroumadi A, Mirzaei SA, Maddahi S, Hassanzadeh SM. In vitro antiparasitic activity and cytotoxic effect of (z)-2-benzylidene-4, 6-dimethoxybenzofuran-3 (2h)-one derivatives. Iran J Parasitol. 2016;11:371.
3. Ramazani A, Zakeri S, Sardari S, Khodakarim N, Djadid ND. In vitro and in vivo anti-malarial activity of boerhavia elegans and solanum surattense. Malar J. 2010;9:124.
4. Heidari A, Keshavarz H. The drug resistance of *Plasmodium falciparum* and *P. Vivax* in Iran: A review article. Iran J Parasitol. 2021;16:173-185.
5. Mahmoudi S, Keshavarz H. Efficacy of phase 3 trial of rts, s/as01 malaria vaccine: The need for an alternative development plan. Hum Vaccin Immunother. 2017;13:2098-2101.
6. Crane EA, Gademann K. Capturing biological activity in natural product fragments by chemical synthesis. Angewandte Chemie International Edition. 2016;55:3882-3902.
7. Jafarpour Azami S, Teimouri A, Keshavarz H et al. Curcumin nanoemulsion as a novel chemical for the treatment of acute and chronic toxoplasmosis in mice. Int J Nanomedicine. 2018; 13:7363-7374.
8. Muthaura C, Keriko J, Dereese S, Yenesew A, Rukungu G. Investigation of some medicinal plants traditionally used for treatment of malaria in Kenya as potential sources of antimalarial drugs. Exp Parasitol. 2011;127:609-626.
9. Robert A, Benoit-Vical F, Dechy-Cabaret O, Meunier B. From classical antimalarial drugs to new compounds based on the mechanism of action of artemisinin. Pure Appl Chem. 2001;73:1173-1188.
10. Simonsen HT, Nordskjold JB, Smitt UW, Nyman U, Palpu P, Joshi P, Varughese G. In vitro screening of indian medicinal plants for antiparasitic activity. J Ethnopharmacol. 2001;74:195-204.
11. Suraveratum N, Krungkrai SR, Leangaramgul P, Prapunwattana P, Krungkrai J. Purification and characterization of *Plasmodium falciparum* succinate dehydrogenase. Mol Biochem Parasitol. 2000;105:215-222.
12. Thiengsusuk A, Chaijaroenkul W, Na-Bangchang K. Antimalarial activities of medicinal plants and herbal formulations used in thai traditional medicine. Parasitol Res. 2013;112:1475-1481.
13. Hsieh YJ, Lin LC, Tsai TH. Measurement and pharmacokinetic study of plumbagin in a conscious freely moving rat using liquid chromatography/tandem mass spectrometry. J Chromatogr B Analyt Technol Biomed Life Sci. 2006;844:1-5.
14. Sharma M, Sharma R, Jain DK, Saraf A. Enhancement of oral bioavailability of poorly water soluble carvedilol by chitosan nanoparticles: Optimization and pharmacokinetic study. Int J Biol Macromol. 2019;135:246-260.
15. Rashidzadeh H, Rezaei SJT, Zamani S, Sarijloo E, Ramazani A. Ph-sensitive curcumin conjugated micelles for tumor triggered drug delivery. J Biomater Sci Polym Ed. 2021;32:320-336.
16. Rezaei SJT, Sarijloo E, Rashidzadeh H, Zamani S, Ramazani A, Hesami A, Mohammadi E. Ph-triggered prodrug micelles for cisplatin delivery: Preparation and in vitro/vivo evaluation. Reactive and Functional Polymers. 2020;146:104399.
17. Fattahi N, Ramazani A, Hamidi M, Parsa M, Rostamizadeh K, Rashidzadeh H. Enhancement of the brain delivery of methotrexate with administration of mid-chain ester prodrugs: In vitro and in vivo studies. Int J Pharm. 2021;600:120479.
18. Nosrati H, Salehiabar M, Bagheri Z, Rashidzadeh H, Davaran S, Danafar H. Preparation, characterization, and evaluation of amino acid modified magnetic nanoparticles: Drug delivery and mri contrast agent applications. Pharm Dev Technol. 2018;23:1156-1167.

19. Somasundaran P, Chin M, Latosiewicz UT, Tuller HL, Barbiellini B, Renugopalakrishnan V. Nanoscience and engineering for robust biosolar cells. In: Bionanotechnology II (pp.427-454). 2011. DOI:10.1201/b11374-23.
20. Kuskov AN, Kulikov PP, Goryachaya AV, Tzatzarakis MN, Tsatsakis AM, Velonia K, Shtilman MI. Self-assembled amphiphilic poly-n-vinylpyrrolidone nanoparticles as carriers for hydrophobic drugs: Stability aspects. *Journal of Applied Polymer Science*. 2018;135:45637.
21. Asadi N, Annabi N, Mostafavi E, Anzabi M, Khalilov R, Saghti S, Mehrizadeh M, Akbarzadeh A. Synthesis, characterization and in vitro evaluation of magnetic nanoparticles modified with pcl-peg-pcl for controlled delivery of 5fu. *Artif Cells Nanomed Biotechnol*. 2018;46:938-945.
22. Ramazani A, Keramati M, Malvandi H, Danafar H, Kheiri Manjili H. Preparation and in vivo evaluation of anti-plasmodial properties of artemisinin-loaded pcl-peg-pcl nanoparticles. *Pharm Dev Technol*. 2018;23:911-920.
23. Rashidzadeh H, Salimi M, Sadighian S, Rostamizadeh K, Ramazani A. In vivo antiplasmodial activity of curcumin-loaded nanostructured lipid carriers. *Curr Drug Deliv*. 2019;16:923-930.
24. Pradeepa V, Senthil-Nathan S, Sathish-Narayanan S, et al. Potential mode of action of a novel plumbagin as a mosquito repellent against the malarial vector *Anopheles stephensi*, (Culicidae: Diptera). *Pestic Biochem Physiol*. 2016;134:84-93.
25. Sumsakul W, Plengsuriyakarn T, Chaijaroenkul W, Viyanant V, Karbwang J, Na-Bangchang K. Antimalarial activity of plumbagin in vitro and in animal models. *BMC Complement Altern Med*. 2014;14:15.
26. Aghajanzadeh M, Zamani M, Rashidzadeh H, Rostamizadeh K, Sharafi A, Danafar H. Amphiphilic y shaped miktoarm star copolymer for anticancer hydrophobic and hydrophilic drugs codelivery: Synthesis, characterization, in vitro, and in vivo biocompatibility study. *J Biomed Mater Res A*. 2018;106:2817-2826.
27. Najer A, Wu D, Nussbaumer MG, et al. An amphiphilic graft copolymer-based nanoparticle platform for reduction-responsive anticancer and antimalarial drug delivery. *Nanoscale*. 2016;8:14858-14869.
28. Kooijmans S, Fliervoet L, Van Der Meel R, et al. Pegylated and targeted extracellular vesicles display enhanced cell specificity and circulation time. *J Control Release*. 2016;224:77-85.
29. Sinlikhitkul N, Toochinda P, Lawtrakul L, Kuropakornpong P, Itharat A. Encapsulation of plumbagin using cyclodextrins to enhance plumbagin stability: Computational simulation, preparation, characterization, and application. *J Incl Phenom Macrocycl Chem*. 2019;93:229-243.
30. Manjili HK, Sharafi A, Danafar H, Hosseini M, Ramazani A, Ghasemi MH. Poly (caprolactone)-poly (ethylene glycol)-poly (caprolactone)(pcl-peg-pcl) nanoparticles: A valuable and efficient system for in vitro and in vivo delivery of curcumin. *Rsc Advances*. 2016;6:14403-14415.
31. Pisal S, Zainnuddin R, Nalawade P, Mahadik K, Kadam S. Drug release properties of polyethylene-glycol-treated ciprofloxacin-indin 234 complexes. *AAPS PharmSciTech*. 2004;5(4):e64.
32. Trivedi R, Kompella UB. Nanomicellar formulations for sustained drug delivery: Strategies and underlying principles. *Nanomedicine*. 2010;5:485-505.
33. Sunil Kumar M, Kiran Aithal B, Udupa N, et al. Formulation of plumbagin loaded long circulating pegylated liposomes: In vivo evaluation in c57bl/6j mice bearing b16f1 melanoma. *Drug Delivery*. 2011;18:511-522.